Atmos. Chem. Phys. Discuss., 15, 24995–25020, 2015
www.atmos-chem-phys-discuss.net/15/24995/2015/
doi:10.5194/acpd-15-24995-2015

Atmospheric Chemistry and Physics Discussions
Open Access

This discussion paper is/has been under review for the journal Atmospheric Chemistry and Physics (ACP). Please refer to the corresponding final paper in ACP if available.

Large XCH_4 anomaly in summer 2013 over Northeast Asia observed by GOSAT

M. Ishizawa[1], O. Uchino[1], I. Morino[1], M. Inoue[1,a], Y. Yoshida[1], K. Mabuchi[1], T. Shirai[1], Y. Tohjima[1], S. Maksyutov[1], H. Ohyama[2], S. Kawakami[3], and A. Takizawa[4]

[1]National Institute for Environmental Studies, Tsukuba, Japan
[2]Solar-Terrestrial Environmental Laboratory, Nagoya University, Nagoya, Japan
[3]Japan Aerospace Exploration Agency, Tsukuba, Japan
[4]Japan Meteorological Agency, Tokyo, Japan
[a]now at: Akita Prefectural University, Akita, Japan

Received: 24 June 2015 – Accepted: 25 August 2015 – Published: 15 September 2015

Correspondence to: M. Ishizawa (ishizawa.misa@nies.go.jp)

Published by Copernicus Publications on behalf of the European Geosciences Union.

Large XCH_4 anomaly in summer 2013 over Northeast Asia observed by GOSAT

M. Ishizawa et. al.

Abstract

Extremely high levels of column-averaged dry-air mole fractions of atmospheric methane (XCH_4) were detected in August and September 2013 over Northeast Asia (∼ 20 ppb above the averaged summertime XCH_4 over 2009–2012, after removing a long-term trend), as being retrieved from the Short-Wavelength InfraRed (SWIR) spectral data observed with the Thermal And Near-infrared Sensor for carbon Observation-Fourier Transform Spectrometer (TANSO-FTS) onboard Greenhouse Gases Observing Satellite (GOSAT). Similar enhancements of XCH_4 were also observed by the ground-based measurements at two Total Carbon Column Observing Network (TCCON) sites in Japan.

The analysis of surface CH_4 concentrations observed at three monitoring sites around the Japan islands suggest that the extreme increase of XCH_4 has occurred in a limited area. The model analysis was conducted to investigate this anomalously high XCH_4 event, using an atmospheric transport model. The results indicate that the extreme increase of XCH_4 is attributed to the anomalous atmospheric pressure pattern over East Asia during the summer of 2013, which effectively transported the CH_4-rich air to Japan from the strong CH_4 source areas in East China. The two Japanese TCCON sites, ∼ 1000 km east-west apart each other, coincidentally located along the substantially CH_4-rich air flow from East China. The GOSAT orbiting with three-day recurrence successfully observed the synoptic-scale XCH_4 enhancement in the comparable accuracy to the TCCON data. This analysis demonstrates the capability of GOSAT to monitor an XCH_4 event on a synoptic scale.

1 Introduction

Atmospheric methane (CH_4) is the second important anthropogenic greenhouse gas after carbon dioxide (CO_2), contributing about 20 % of the total radiative forcing from the major well-mixed greenhouse gases (Forster et al., 2007). Methane has multiple natural and anthropogenic sources in the Earth's surface while being mainly removed through reaction with hydroxyl radical (OH) in the troposphere and by photolysis in the stratosphere. The atmospheric CH_4 level has more than doubled since the onset of the industrial revolution in the 18th century (Etheridge et al., 1998). Its growth rate has been considerably variable over the past few decades (Dlugokencky et al., 2009). On a global scale, the causes of recent changes in the CH_4 growth rate remain unknown (e.g. Kirschke et al., 2013; Dlugokencky et al., 2009), and on a regional scale, significant discrepancies have been found in the emission estimates between bottom-up and top-down approaches (e.g. Miller et al., 2013). On the other hand, given the larger radiative forcing than carbon dioxide, it has been argued that reducing anthropogenic CH_4 emission might be a mitigation of possible severe impact of global warming (e.g. Hansen and Sato, 2004). Therefore, to elucidate the drivers of changes in atmospheric CH_4 concentrations and to quantify the regional source distributions are challenging tasks.

The temporal variations of observed atmospheric CH_4 are complicated due to various sources on the Earth surface, interactions between the emission sources and the atmospheric transport, and removal in the atmosphere. To improve the regional CH_4 flux estimates on the Earth surface, it is needed to better understand the relative contribution of atmospheric transport to the observed variations of atmospheric CH_4.

In the past decades, the investigations of the spatiotemporal variability in atmospheric CH_4 concentrations and the inverse modeling of surface CH_4 flux estimates had been mainly based on the ground-based measurements (e.g. Bousquet et al., 2006; Bergamaschi et al., 2010; Miller et al., 2013). However, the current ground-based measurements of CH_4 are still sparse. In the recent years, the measurements from the satellites have been providing the large spatial and temporal coverage to help better understand the variations of atmospheric CH_4. Since 2009, Greenhouse gases Observing SATellite (GOSAT) has been provided column-averaged dry-air mole fractions of atmospheric CH_4 (XCH_4) that are retrieved from Short-Wavelength InfraRed (SWIR) solar spectra observed onboard Thermal And Near infrared Sensor for carbon

ACPD
15, 24995–25020, 2015

Observation-Fourier Transform Spectrometer (TANSO-FTS) instrument (Yokota et al., 2009; Yoshida et al., 2013). GOSAT XCH_4 is preceded by the several previous and on-going satellite projects, for example, the Infrared Atmospheric Sounding Interferometer (IASI, Crevoisier et al., 2009), and the Tropospheric Emission Spectrometer (TES, Wecht et al., 2012) and the SCanning Imaging Absorption spectroMeter for Atmospheric CHartographY (SCIAMACHY, Schneising et al., 2011). Among them, XCH_4 retrievals from SCIAMACHY instrument onboard ENVISAT launched in 2003 was pioneering, but the communication with ENVISAT was lost in April 2012. The GOSAT TANSO-FTS aims at providing measurements of atmospheric CH_4 concentrations in three-month averages with an accuracy of higher than 2 % at 100–1000 km spatial resolution (Kuze et al., 2009).

Here, we report the extremely high XCH_4 event observed by GOSAT in August and September 2013 over Northeast Asia. Similar high XCH_4 event were also detected by the ground-based measurements at the two Japanese Total Carbon Column Observing Network (TCCON) sites in Tsukuba and Saga. Given the spacing and temporal frequency (three-day recurrence) of GOSAT sampling, along with possible retrieval biases of XCH_4 retrievals, it is interesting that the GOSAT detected the synoptic-scale variation of XCH_4 that is coherent with the ground-based measurements. This GOSAT-detected XCH_4 event suggests the potential of GOSAT XCH_4 analysis in higher temporal and spatial resolution. In this study, we analyse the observed extremely high GOSAT XCH_4 in the summer of 2013 to investigate the attributions of such a significant increase of XCH_4. As charactering the observed extreme event of atmospheric CH_4 in terms of spatial extent and temporal duration, we also discuss how capable GOSAT XCH_4 monitors synoptic-scale XCH_4 variations.

ACPD
15, 24995–25020, 2015

2 Observations

2.1 GOSAT XCH_4

GOSAT is a joint project of the Japanese Ministry of the Environment (MOE), the National Institute for Environmental Studies (NIES) and the Japan Aerospace Exploration Agency (JAXA) to monitor the global distribution of atmospheric CO_2 and CH_4 from space (Yokota et al., 2009). The retrieved XCH_4, as a part of NIES GOSAT Level 2 (L2) product (v02.xx), has been reported to have a mean bias of −5.9 ppb and mean standard deviation of 12.6 ppb against the XCH_4 at selected TCCON sites (Yoshida et al., 2013). In this study, we analysed NIES GOSAT L2 XCH_4 (v02.21) without any bias correction. The description of the latest updated retrieval procedures and the auxiliary information can be found at GOSAT User Interface Gateway (https://data.gosat.nies.go.jp).

We analysed GOSAT XCH_4 over two regions in Northeast Asia separately (Fig. 1). One is over northeastern China-Korea (115–130° E, 30–40° N), and the other is over Japan (130–145° E, 30–40° N). The northeastern China-Korea region covers highly populated and industrialized areas with large anthropogenic CH_4 sources in the Eurasia continent. The Japan region has small CH_4 sources, but located downwind of the continental CH_4 emissions. Time-series of all the XCH_4 data from June 2009 to March 2014 over the two regions with monthly means are shown in Fig. 2. It is noted that we used only the XCH_4 over land to minimize possible errors depending on sounding observation mode. In fact, since a few soundings over ocean around East Asia were retrieved, removed XCH_4 data through this criterion are less than 5 % of the total. A long-term trend component in each XCH_4 dataset derived through a digital filtering of two-year cutoff period (Nakazawa et al., 1997) is also plotted in Fig. 2. To focus the seasonal variations, the trend components were removed, and the detrended XCH_4 time-series are further analysed.

The GOSAT XCH_4 retrievals over Northeastern China-Korea have clear seasonality with high peaks in summer and low peaks in winter. The summertime high XCH_4 must

Discussion Paper | Discussion Paper | Discussion Paper | Discussion Paper |
ACPD
15, 24995–25020, 2015
Large XCH_4 anomaly in summer 2013 over Northeast Asia observed by GOSAT
M. Ishizawa et. al.

be partially attributed to the seasonal biogenic CH_4 emissions from rice paddies and natural wetlands underneath in East China and Korea. The summer peak in 2013 was more prominent than the preceding two years, 2011 and 2012. Also, the summertime XCH_4 retrievals over Northeastern China-Korea in 2009 and 2010 were relatively high while no significantly high XCH_4 was observed over Japan. Since there is a limited number of retrieval available over Japan for the first two years of the GOSAT operation, it is difficult to discuss the XCH_4 difference over the two regions for 2009 and 2010. We thus leave this topic for a future investigation.

The seasonality of the GOSAT XCH_4 retrieval over Japan is overall similar to Northeastern China-Korea. Although the seasonal cycle varies largely year-to-year, XCH_4 retrievals of August and September in 2013 were outstandingly high. Japan is located downwind of strong anthropogenic and natural biogenic CH_4 emissions in the continent, and then the signals of the continental CH_4 emissions are lowered as the air is transported. However, it is noticeable that, in the summer of 2013, the XCH_4 retrievals over both Japan and Northeastern China-Korea regions reached the almost same high levels. This comparable XCH_4 levels in the two regions indicates there was a mechanism of fast atmospheric transport in 2013 to bring CH_4-rich air to Japan with less diffusion than the preceding years.

2.2 TCCON XCH_4

Inside the Japan region of this study, ground-based XCH_4 measurements have been conducted at two TCCON sites, Saga (33.24° N, 130.29° E) and Tsukuba (36.05° N, 140.12° E) as shown in Fig. 1. TCCON is a worldwide network of ground-based high-resolution FTSs, which record spectra of the direct sunlight in the near-infrared, and provides accurate and precise column-averaged dry-mole fractions of atmospheric constituents including CO_2, CH_4, N_2O, HF, CO, H_2O, and HDO retrieved from these spectra absorbed by them (Wunch et al., 2011). The TCCON XCH_4 measurements have an estimated uncertainty of 7 ppb (2σ) (Wunch et al., 2010). TCCON data play a critical role in the validation of space-based measurements. The Saga TCCON site

ACPD
15, 24995–25020, 2015

is in Kyushu Island, operated by JAXA since June 2011. The Tsukuba TCCON site is located ∼ 50 km north of Tokyo in the Japan main island, operated by NIES since 2009. These two Japanese TCCON sites are apart ∼ 1000 km longitudinally.

Figure 3 shows XCH_4 retrievals at Saga and Tsukuba TCCON sites during the period for 2011 to 2014. We processed the both TCCON XCH_4 time-series in the same manner with the GOSAT XCH_4 to obtain the long-term trends that are shown in blue lines in Fig. 3. It is interesting that, before the summer 2013, XCH_4 retrievals at Tsukuba overall are lower than at Saga. Since Saga is located closer to the continent than Tsukuba, Saga is considered to be influenced by the continental anthropogenic CH_4 emissions more strongly than Tsukuba. In the summer of 2013, extremely high XCH_4 retrievals both at Saga and Tsukuba were observed, reaching almost a same level. This XCH_4 enhancement observed at the ground-based TCCON sites is coincident with the high XCH_4 observed by GOSAT, and strongly supports our speculation that the CH_4 rich air was transported quickly from the continent to Japan for this period.

To focus on the seasonal and synoptic variations, we compared the detrended XCH_4 time-series from GOSAT over Japan and the two Japanese TCCON sites. Figure 4 shows that all the detrended XCH_4 data agree overall with each other in the timing of seasonal cycle. Compared with TCCON XCH_4, GOSAT XCH_4 shows large short-term variability, but has small seasonal amplitude of ∼ 10 ppb. In 2012, both GOSAT XCH_4 and TCCON XCH_4 were highly variable, but not clear tendency in August. In September 2012, TCCON XCH_4 at the two sites increased together by ∼ 10 ppb while the increase of GOSAT XCH_4 was not clearly seen. In 2013, both GOSAT and TCCON XCH_4 together rapidly increased in August and remained high in September. The averages of all detrended XCH_4 for August and September 2013 are higher by ∼ 20 ppb than the XCH_4 levels for 2012. This enhancement of GOSAT XCH_4 over Japan is roughly double of its average seasonal amplitude.

ACPD
15, 24995–25020, 2015

2.3 Ground-based surface CH_4 concentrations

In order to see the relationship between the surface CH_4 concentration and the enhancement of GOSAT XCH_4 over Japan, we analyzed the surface CH_4 concentrations observed at three ground-based monitoring stations in Japan, Cape Ochi-ishi (COI, 43.16° N, 145.49° E), Ryori (RYO, 39.03° N, 141.82° E), and Yonagunijima (YON, 24.47° N, 123.02° E). These site locations are shown in Fig. 1. At all the stations, continuous measurements of atmospheric CH_4 are conducted. Cape Ochi-ishi (COI) is a station operated by NIES, which is located at the east tip of Hokkaido island (Tohjima et al., 2002). Ryori (RYO) is located inside the Japan region defined in this study, where the monitoring of surface greenhouse gas concentrations has been conducted by the Japan Meteorological Agency (JMA) as a part of the Global Atmospheric Watch (GAW) program of the World Meteorological Observation (WMO). RYO is on the west coast of the Japan main island, about 300 km north of Tsukuba and far away from direct influences of residential and industrial pollutants. Yonagunijima (YON) is also one of JMA-operated GAW stations, which is located far south of the Japan main island and east of ~ 110 km of Taiwan. The details on RYO and YON are provided on the web page of WMO GAW World Data Centre for Greenhouse Gases (WDCGG) (http://ds.data.jma.go.jp/gmd/wdcgg/introduction.html).

The time-series of surface CH_4 concentrations at the three ground-based stations are shown in Fig. 5, with their monthly means and long-term trends. Here we analyzed the afternoon mean CH_4 (averaged hourly CH_4 over 12:00–15:00 LT) from the respective data sets, assuming that the afternoon values are large-scale representative. The observed CH_4 concentrations at all the sites show similar seasonal cycles in timing. Seasonally the CH_4 values are low in July and August, and high in winter to spring. In the winter, the westerly wind prevails and transports the CH_4-rich air from the continent (mainly anthropogenic CH_4 emitted in East China) to Japan, causing the rise of CH_4 concentrations. In the summer, the southeasterly wind is dominant, bringing clean air

ACPD
15, 24995–25020, 2015

to Japan from the Pacific Ocean, where is no major CH_4 source, so that the surface CH_4 concentrations become low.

In the summer of 2013, unseasonably high CH_4 concentrations were observed at RYO with a sharp increase in the middle of August. The CH_4 concentrations at COI started increasing earlier from its summer minimum than the previous year, 2012. At YON, no significant CH_4 enhancement was seen in 2013 compared with the previous years. Since no similar CH_4 change to RYO and COI was observed at YON, the farthest southwestern island of Japan, this significant CH_4 enhancement event appears to be spatially limited in the area around Japan main island and Hokkaido island. To further examine the summer increase of surface CH_4 concentrations, we compared the detrended CH_4 at RYO and COI for the two years of 2012 and 2013 (Fig. 6). The timing and amplitude of seasonal cycles at RYO and COI overall agree well with each other, except for the summer of 2013. In August and September 2013, the temporal variations of CH_4 at RYO and COI are different from those in the previous year 2012 when the CH_4 concentrations were low over the summertime and started rising at the end of September. In August 2013, the abrupt CH_4 increase by ∼ 100 ppb was observed at RYO, followed by COI with ∼ 1 week delay. In September, the CH_4 at both sites lowered but stayed in the higher level than 2012. Given that the fact the major CH_4 sources in East China, the sudden large increase of CH_4 in August 2013 is probably caused by unseasonal transport of CH_4-rich air from the continent to Japan though normally in August the wind with CH_4-low air from the Pacific Ocean is prevailing over Japan.

3 Model analysis

The observational data analysis suggested that the atmospheric transport would be a key factor of the extreme enhancement event of XCH_4 and surface CH_4 concentrations in the summer of 2013 over Japan. To investigate how the inter-annually varying atmospheric transport plays the role in the enhancement of XCH_4 and surface CH_4, we

ACPD
15, 24995–25020, 2015

conducted a forward model simulation using the global atmospheric transport model of National Institute for Environmental Studies (NIES-TM) version 8.1i.

The NIES-TM has a horizontal resolution of $2.5^\circ \times 2.5^\circ$ with 32 vertical layers (Belikov et al., 2013). The global wind fields used in this study were obtained from the JMA Climate Data Assimilation System (JCDAS) (Onogi et al., 2007). The planetary boundary layer height data are obtained from the European Centre for Medium-Range Weather Forecasts (ECMWF) Interim Reanalysis dataset (Dee et al., 2011). In order to examine the impact of time-varying atmospheric transport on the seasonal cycles of atmospheric CH_4 and XCH_4 fields, the CH_4 emissions averaged over 2009–2010 were repeatedly used during the entire model simulation period for 2009–2013. The CH_4 emissions comprise anthropogenic fluxes and natural fluxes. The anthropogenic fluxes are from the Emissions Database for Global Atmospheric Research (EDGAR) inventory, v4.2 FT2010 (http://edgar.jrc.ec.europa.eu/). The natural CH_4 fluxes are biomass burning from Global Fire Emissions Database (GFED) v3.1 (van der Werf et al., 2010), wetland, rice paddy emissions and soil sinks from the Vegetation Integrative Simulator for Trace gases (VISIT) (Ito and Inatomi, 2012), and termites (Fung et al., 1991). Except the termites CH_4 emission, all the natural fluxes are seasonal. We used the modeled methane loss and climatological OH fields provided for a model inter-comparison project "TransCom-CH_4" (Patra et al., 2011).

Figure 7 shows the simulated surface CH_4 concentration and XCH_4 fields for August and September in 2012 and 2013. Both fields are plotted with respect to the surface CH_4 concentration and XCH_4 at the South Pole to examine the inter-annual variations, removing the long-term trends in the model simulations. As a common feature, the high levels of XCH_4 and surface CH_4 are found over East China, reflecting the spatial distribution of the strong anthropogenic emissions around Beijing and Shanghai and biogenic CH_4 sources from rice cultivation in the southeastern China.

Different patterns are found in the XCH_4 and surface CH_4 fields between 2012 and 2013. In August 2012, both levels of XCH_4 and surface CH_4 over Japan are as low as those over the Pacific oceans. In August 2013, higher concentrations of surface CH_4

ACPD
15, 24995–25020, 2015

extended from the northeastern China and the Korean peninsula to the Japan islands. The surface CH_4 concentration level in 2013 over Japan is increased by 40–60 ppb from the level in 2012. The XCH_4 values over Japan are also enhanced by $\sim$ 30 ppb while the XCH_4 values over East China coast are lowered compared to the 2012 level. These simulated enhancements of XCH_4 and CH_4 concentration over Japan are comparable to the observations (Figs. 4 and 6). The lower concentrations in August 2013 over East China than 2012 indicate that the wind was so fast that CH_4 was not much accumulated over the CH_4 source area, but transported away. In September 2013, XCH_4 level over East China became higher than August, but still lower than the level of September of 2012. Also the XCH_4 over Japan remains higher level than that of 2012. The surface CH_4 concentration pattern in September 2013 is almost similar to the one in 2012, but slightly higher values are found over Japan. This model exercise indicates the inter-annual variation of atmospheric transport would be the key to the large anomalies of XCH_4 and CH_4 concentrations over Japan in the summer of 2013.

4 Discussions

4.1 Characteristics of atmospheric circulation in the summer of 2013

Forward modeling gives us insights into the contribution of atmospheric transport on the enhancement of XCH_4 and surface CH_4 concentration in the summer of 2013 over Japan. Here we examine the 2013 summertime atmospheric transport over the north-eastern Asia.

Japan's summer climate is governed by the Pacific High (a lower-level high-pressure system) and the Tibetan High (an upper-level high-pressure system). These pressure systems were reported to have been enhanced during July and August 2013 (Tokyo Climate Center News No.34 Autumn 2013, available at http://ds.data.jma.go.jp/tcc/tcc/news). The Pacific High continued to expand westward and largely developed over the western part of Japanese islands including Okinawa. The Tibetan High expanded to the

Japan main island in line with the northward meandering of upper-level westerly winds (the subtropical jet stream). The enhanced atmospheric transport from East China to Japan was probably attributed to those anomalously developed high-pressure systems.

To see how the 2013 summertime atmospheric transport differs from the mean transport pattern, Fig. 8 shows the wind fields at the surface and at 850 hPa pressure level, from the JCDAS wind fields of August and September in 2013 over East Asia, compared with those of the mean wind fields for the five years of 2009–2013.

At the surface level (Fig. 8a), the mean wind field clearly shows that, in August the southeasterly wind from the Pacific Ocean prevails as a result of the development of the Pacific High. In September the wind from the continent to Japan start blowing as the Pacific High is retiring. In August 2013, as the Pacific High expanded westward, the air moved northward along the coast of China, turned around the Korean Peninsula, and flowed to Japan. This wind pattern suggests that the CH_4-rich air was transported from East China to Japan in 2013, while the clean air is normally transported from the Pacific Ocean. In September 2013, over the Pacific Ocean, south of the Japan main island, easterly wind was still stronger than the normal, but the wind pattern over Japan was almost back to the normal, which can be characterized as a weak convergence of westerly wind from the continent and easterly wind from the Pacific Ocean. This nearly normal wind pattern over northern Japan would lower the CH_4 concentrations at the surface level as observed at RYO and COI.

At the 850 hPa level (Fig. 8b), it is notable that, in August 2013 the air moved over the East China along the coast and turned around the Korean peninsula sharply to the Japan islands. The anomalous westerly winds were stronger in the upper levels than near the surface. Given the major CH_4 source distributions in East Asia, the strong northward air flow along the coast could reduce local CH_4 accumulation, but transport the CH_4-rich air effectively to the north and then to Japan as turning around the Korean peninsula. In September 2013, the wind speed over Japan was much lower than August, but wind still blows westerly from the continent to Japan. This westerly air flow could maintain the higher level of XCH_4 over Japan during the September of 2013.

ACPD
15, 24995–25020, 2015

4.2 Other possible factors

Although we suggest that the atmospheric transport field probably attributes to the enhancement of XCH_4 and CH_4 concentration observed in the summer of 2013, we cannot entirely rule out other possible factors. CH_4 emissions from rice cultivations and wetland in Southern China might be enhanced under the hot summer condition in 2013. East Asia around China experienced a hotter summer monsoon season (June–September) by more than 1 °C than the season normal (Tokyo Climate Center News No.34 Autumn 2013), while less than 60 % of the normal precipitation in eastern China was reported. A hot weather condition increases the CH_4 emissions through the enhancement of photosynthesis and methanogenic activity in inundated grounds such as wetlands and rice paddies; while a dry condition reduces the CH_4 emissions from wetlands as the water table levels in the ground become low. Thus, the hot and dry weather conditions have opposite effects on the CH_4 emissions from wetlands. The time delay in the correlation between CH_4 emissions and climate anomalies should be considered as the groundwater plays an important role in wetland CH_4 emissions. Furthermore, since rice cultivation is human-managed, multiple controlling factors on CH_4 emissions from rice paddies should be considered. A further investigation of wetland and rice CH_4 emission changes responding to the climate anomaly in East Asia is needed.

5 Conclusions

In this study, we have examined the synoptic-scale extremely high XCH_4 event over Northeast Asia observed by GOSAT in August and September 2013. Similar XCH_4 enhancements in amplitude and timing were observed at the two Japanese TCCON sites, Tsukuba and Saga. Furthermore, during the same period, the ground-based atmospheric CH_4 monitoring sites of Ryori and Ochi-ishi located in the northern part of

ACPD
15, 24995–25020, 2015

Japan observed the higher levels of surface CH_4. In particular, surface CH_4 concentrations at Ryori showed the rapid increase in the middle of August 2013.

Our model analysis indicates that the large enhancement of XCH_4 and surface CH_4 are mainly attributed to the anomalous atmospheric pressure patterns of Pacific High and Tibetan High over East Asia during the summer of 2013. The CH_4-rich air effectively was transported to Japan from the major CH_4 source area in East China. The model analysis also indicates that the XCH_4 enhancement occurred in a limited area of North China to the Japan main island. The two Japanese TCCON sites, ~ 1000 km apart from each other, happened to be located along the anomalously CH_4-rich air flow from the Eurasian continent, and coincidentally observed the extreme increase of XCH_4. The GOSAT orbiting with three-day recurrence successfully observed the large XCH_4 anomaly event. This data analysis study demonstrates the capability of space-based observation by GOSAT to monitor an XCH_4 event on a synoptic scale in the association with the high-pressure system anomalies in the comparable accuracy with ground-based observations. This GOSAT capability regarding synoptic-scale variations could be helpful to quantify the relative contribution of atmospheric transport toward better estimates of regional CH_4 fluxes.

Acknowledgements. Surface CH_4 data observed at Ryori and Yonagunijima are got from the WDCGG (http://ds.data.jma.go.jp/gmd/wdcgg/). CCON data were obtained from the TCCON Data Archive, operated by the California Institute of Technology from the website at tccon.ipac.caltech.edu.

References

Belikov, D. A., Maksyutov, S., Sherlock, V., Aoki, S., Deutscher, N. M., Dohe, S., Griffith, D., Kyro, E., Morino, I., Nakazawa, T., Notholt, J., Rettinger, M., Schneider, M., Sussmann, R., Toon, G. C., Wennberg, P. O., and Wunch, D.: Simulations of column-averaged CO_2 and CH_4 using the NIES TM with a hybrid sigma-isentropic (σ–θ) vertical coordinate, Atmos. Chem. Phys., 13, 1713–1732, doi:10.5194/acp-13-1713-2013, 2013.

Bergamaschi, P., Krol, M., Meirink, J. F., Dentener, F., Segers, A., van Aardenne, J., Monni, S., Vermeulen, A. T., Schmidt, M., Ramonet, M., Yver, C., Meinhardt, F., Nisbet, E. G., Fisher, R. E., O'Doherty, S., and Dlugokencky, E. J.: Inverse modeling of European CH_4 emissions 2001–2006, J. Geophys. Res., 115, D22309, doi:10.1029/2010JD014180, 2010.

Bousquet, P., Ciais, P., Miller, J. B., Dlugokencky, E. J., Hauglustaine, D. A., Prigent, C., Van der Werf, G. R., Peylin, P., Brunke, E. G., Carouge, C., Langenfelds, R. L., Lathiere, J., Papa, F., Ramonet, M., Schmidt, M., Steele, L. P., Tyler, S. C., and White, J.: Contribution of anthropogenic and natural sources to atmospheric methane variability, Nature, 443, 439–443, doi:10.1038/nature05132, 2006.

Crevoisier, C., Nobileau, D., Fiore, A. M., Armante, R., Chédin, A., and Scott, N. A.: Tropospheric methane in the tropics – first year from IASI hyperspectral infrared observations, Atmos. Chem. Phys., 9, 6337–6350, doi:10.5194/acp-9-6337-2009, 2009.

Dee, D. P., Uppala, S. M., Simmons, A. J., Berrisford, P., Poli, P., Kobayashi, S., Andrae, U., Balmaseda, M. A., Balsamo, G., Bauer, P., Bechtold, P., Beljaars, A. C. M., van de Berg, L., Bidlot, J., Bormann, N., Delsol, C., Dragani, R., Fuentes, M., Geer, A. J., Haimberger, L., Healy, S. B., Hersbach, H., Hólm, E. V., Isaksen, L., Kållberg, P., Köhler, M., Matricardi, M., McNally, A. P., Monge-Sanz, B. M., Morcrette, J. J., Park, B. K., Peubey, C., de Rosnay, P., Tavolato, C., Thépaut, J. N., and Vitart, F.: The ERA-Interim reanalysis: configuration and performance of the data assimilation system, Q. J. Roy. Meteor. Soc., 137, 553–597, doi:10.1002/qj.828, 2011.

Dlugokencky, E. J., Bruhwiler, L., White, J. W. C., Emmons, L. K., Novelli, P. C., Montzka, S. A., Masarie, K. A., Lang, P. M., Crotwell, A. M., Miller, J. B., and Gatti, L. V.: Observational constraints on recent increases in the atmospheric CH_4 burden, Geophys. Res. Lett., 36, L18803, doi:10.1029/2009GL039780, 2009.

Etheridge, D. M., Steele, L. P., Francey, R. J., and Langenfelds, R. L.: Atmospheric methane between 1000 AD and present: evidence of anthropogenic emissions and climatic variability, J. Geophys. Res., 103, 15979–15993, doi:10.1029/98JD00923, 1998.

Forster, P., Ramaswamy, V., Artaxo, P., Berntsen, T., Betts, R., Fahey, D. W., Haywood, J., Lean, J., Lowe, D. C., Myhre, G., Nganga, J., Prinn, R., Raga, G., Schulz, M., and Van Dorland, R.: Changes in atmospheric constituents and in radiative forcing, in: Climate Change 2007: The Physical Science Basis. Contribution of Working Group I to the Fourth Assessment Report of the Intergovernmental Panel on Climate Change, edited by: Solomon, S.,

Qin, D., Manning, M., Chen, Z., Marquis, Averyt, K. B., Tignor, M., and Miller, H. L., Cambridge University Press, Cambridge, UK and New York, USA, 129–234, 2007.
Fung, I., John, J., Lerner, J., Matthews, E., Prather, M., Steele, L. P., and Fraser, P. J.: Three-dimensional model synthesis of the global methane cycle, J. Geophys. Res., 96, 13033–13065, doi:10.1029/91JD01247, 1991.
Hansen, J. and Sato, M.: Greenhouse gas growth rates, P. Natl. Acad. Sci. USA, 101, 16109–16114, doi:10.1073/pnas.0406982101, 2004.
Ito, A. and Inatomi, M.: Use of a process-based model for assessing the methane budgets of global terrestrial ecosystems and evaluation of uncertainty, Biogeosciences, 9, 759–773, doi:10.5194/bg-9-759-2012, 2012.
Kirschke, S., Bousquet, P., Ciais, P., Saunois, M., Canadell, J. G., Dlugokencky, E. J., Bergamaschi, P., Bergmann, D., Blake, D. R., Bruhwiler, L., Cameron-Smith, P., Castaldi, S., Chevallier, F., Feng, L., Fraser, A., Heimann, M., Hodson, E. L., Houweling, S., Josse, B., Fraser, P. J., Krummel, P. B., Lamarque, J.-F., Langenfelds, R. L., Le Quéré, C., Naik, V., O'Doherty, S., Palmer, P. I., Pison, I., Plummer, D., Poulter, B., Prinn, R. G., Rigby, M., Ringeval, B., Santini, M., Schmidt, M., Shindell, D. T., Simpson, I. J., Spahni, R., Steele, L. P., Strode, S. A., Sudo, K., Szopa, S., van der Werf, G. R., Voulgarakis, A., van Weele, M., Weiss, R. F., Williams, J. E., and Zeng, G.: Three decades of global methane sources and sinks, Nat. Geosci., 6, 813–823, doi:10.1038/ngeo1955, 2013.
Kuze, A., Suto, H., Nakajima, M., and Hamazaki, T.: Thermal and near infrared sensor for carbon observation Fourier-transform spectrometer on the Greenhouse Gases Observing Satellite for greenhouse gases monitoring, Appl. Optics, 48, 6716–6733, doi:10.1364/AO.48.006716, 2009.
Miller, S. M., Wofsy, S. C., Michalak, A. M., Kort, E. A., Andrews, A. E., Biraud, S. C., Dlugokencky, E. J., Eluszkiewicz, J., Fischer, M. L., Janssens-Maenhout, G., Miller, B. R., Miller, J. B., Montzka, S. A., Nehrkorn, T., and Sweeney, C.: Anthropogenic emissions of methane in the United States, P. Natl. Acad. Sci. USA, 110, 20018–20022, doi:10.1073/pnas.1314392110, 2013.
Nakazawa, T., Ishizawa, M., Higuchi, K., and Trivett, N. B. A.: Two curve fitting methods applied to CO_2 flask data, Environmetrics, 8, 197–218, 1997.
Onogi, K., Tsutsui, J., Koide, H., Sakamoto, M., Kobayashi, S., Hatsushika, H., Matsumoto, T., Yamazaki, N., Kamahori, H., Takahashi, K., Kadokura, S., Wada, K., Kato, K., Oyama, R.,

ACPD
15, 24995–25020, 2015

Ose, T., Mannoji, N., and Taira, R.: The JRA-25 Reanalysis, J. Meteorol. Soc. Jpn., 85, 369–432, doi:10.2151/jmsj.85.369, 2007.

Patra, P. K., Houweling, S., Krol, M., Bousquet, P., Belikov, D., Bergmann, D., Bian, H., Cameron-Smith, P., Chipperfield, M. P., Corbin, K., Fortems-Cheiney, A., Fraser, A., Gloor, E., Hess, P., Ito, A., Kawa, S. R., Law, R. M., Loh, Z., Maksyutov, S., Meng, L., Palmer, P. I., Prinn, R. G., Rigby, M., Saito, R., and Wilson, C.: TransCom model simulations of CH_4 and related species: linking transport, surface flux and chemical loss with CH_4 variability in the troposphere and lower stratosphere, Atmos. Chem. Phys., 11, 12813–12837, doi:10.5194/acp-11-12813-2011, 2011.

Schneising, O., Buchwitz, M., Reuter, M., Heymann, J., Bovensmann, H., and Burrows, J. P.: Long-term analysis of carbon dioxide and methane column-averaged mole fractions retrieved from SCIAMACHY, Atmos. Chem. Phys., 11, 2863–2880, doi:10.5194/acp-11-2863-2011, 2011.

Tanaka, T., Miyamoto, Y., Morino, I., Machida, T., Nagahama, T., Sawa, Y., Matsueda, H., Wunch, D., Kawakami, S., and Uchino, O.: Aircraft measurements of carbon dioxide and methane for the calibration of ground-based high-resolution Fourier Transform Spectrometers and a comparison to GOSAT data measured over Tsukuba and Moshiri, Atmos. Meas. Tech., 5, 2003–2012, doi:10.5194/amt-5-2003-2012, 2012.

Tohjima, Y., Machida, T., Utiyama, M., Katsumoto, M., Fujinuma, Y., and Maksyutov, S.: Analysis and presentation of in situ atmospheric methane measurements from Cape Ochi-ishi and Hateruma Island, J. Geophys. Res., 107, ACH 8-1-ACH 8-11, doi:10.1029/2001JD001003, 2002.

van der Werf, G. R., Randerson, J. T., Giglio, L., Collatz, G. J., Mu, M., Kasibhatla, P. S., Morton, D. C., DeFries, R. S., Jin, Y., and van Leeuwen, T. T.: Global fire emissions and the contribution of deforestation, savanna, forest, agricultural, and peat fires (1997–2009), Atmos. Chem. Phys., 10, 11707–11735, doi:10.5194/acp-10-11707-2010, 2010.

Wecht, K. J., Jacob, D. J., Wofsy, S. C., Kort, E. A., Worden, J. R., Kulawik, S. S., Henze, D. K., Kopacz, M., and Payne, V. H.: Validation of TES methane with HIPPO aircraft observations: implications for inverse modeling of methane sources, Atmos. Chem. Phys., 12, 1823–1832, doi:10.5194/acp-12-1823-2012, 2012.

Wunch, D., Toon, G. C., Wennberg, P. O., Wofsy, S. C., Stephens, B. B., Fischer, M. L., Uchino, O., Abshire, J. B., Bernath, P., Biraud, S. C., Blavier, J.-F. L., Boone, C., Bowman, K. P., Browell, E. V., Campos, T., Connor, B. J., Daube, B. C., Deutscher, N. M., Diao, M.,

ACPD
15, 24995–25020, 2015

Large XCH_4 anomaly in summer 2013 over Northeast Asia observed by GOSAT

M. Ishizawa et. al.

Elkins, J. W., Gerbig, C., Gottlieb, E., Griffith, D. W. T., Hurst, D. F., Jiménez, R., Keppel-Aleks, G., Kort, E. A., Macatangay, R., Machida, T., Matsueda, H., Moore, F., Morino, I., Park, S., Robinson, J., Roehl, C. M., Sawa, Y., Sherlock, V., Sweeney, C., Tanaka, T., and Zondlo, M. A.: Calibration of the Total Carbon Column Observing Network using aircraft profile data, Atmos. Meas. Tech., 3, 1351–1362, doi:10.5194/amt-3-1351-2010, 2010.

Wunch, D., Wennberg, P. O., Toon, G. C., Connor, B. J., Fisher, B., Osterman, G. B., Frankenberg, C., Mandrake, L., O'Dell, C., Ahonen, P., Biraud, S. C., Castano, R., Cressie, N., Crisp, D., Deutscher, N. M., Eldering, A., Fisher, M. L., Griffith, D. W. T., Gunson, M., Heikkinen, P., Keppel-Aleks, G., Kyrö, E., Lindenmaier, R., Macatangay, R., Mendonca, J., Messerschmidt, J., Miller, C. E., Morino, I., Notholt, J., Oyafuso, F. A., Rettinger, M., Robinson, J., Roehl, C. M., Salawitch, R. J., Sherlock, V., Strong, K., Sussmann, R., Tanaka, T., Thompson, D. R., Uchino, O., Warneke, T., and Wofsy, S. C.: A method for evaluating bias in global measurements of CO_2 total columns from space, Atmos. Chem. Phys., 11, 12317–12337, doi:10.5194/acp-11-12317-2011, 2011.

Yokota, T., Yoshida, Y., Eguchi, N., Ota, Y., Tanaka, T., Watanabe, H., and Maksyutov, S.: Global concentrations of CO_2 and CH_4 retrieved from GOSAT: First preliminary results, SOLA, 5, 160–163, doi:10.2151/sola.2009-041, 2009.

Yoshida, Y., Kikuchi, N., Morino, I., Uchino, O., Oshchepkov, S., Bril, A., Saeki, T., Schutgens, N., Toon, G. C., Wunch, D., Roehl, C. M., Wennberg, P. O., Griffith, D. W. T., Deutscher, N. M., Warneke, T., Notholt, J., Robinson, J., Sherlock, V., Connor, B., Rettinger, M., Sussmann, R., Ahonen, P., Heikkinen, P., Kyrö, E., Mendonca, J., Strong, K., Hase, F., Dohe, S., and Yokota, T.: Improvement of the retrieval algorithm for GOSAT SWIR XCO_2 and XCH_4 and their validation using TCCON data, Atmos. Meas. Tech., 6, 1533–1547, doi:10.5194/amt-6-1533-2013, 2013.

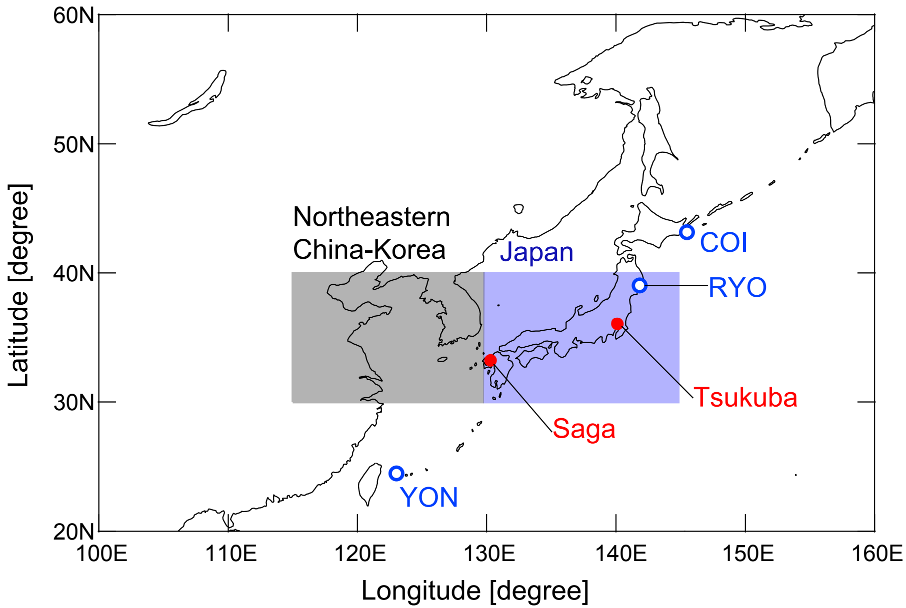

Figure 1. Two regions considered in this study: Northeastern China-Korea (115–130° E, 30–40° N, gray-shaded) and Japan (130–145° E, 30–40° N, blue-shaded). The locations of the Saga and Tsukuba TCCON stations are marked by closed circles. The open circles are indicated the locations of the surface monitoring stations around Japan, Cape Ochi-ishi (COI), Ryori (RYO), and Yonagunijima (YON).

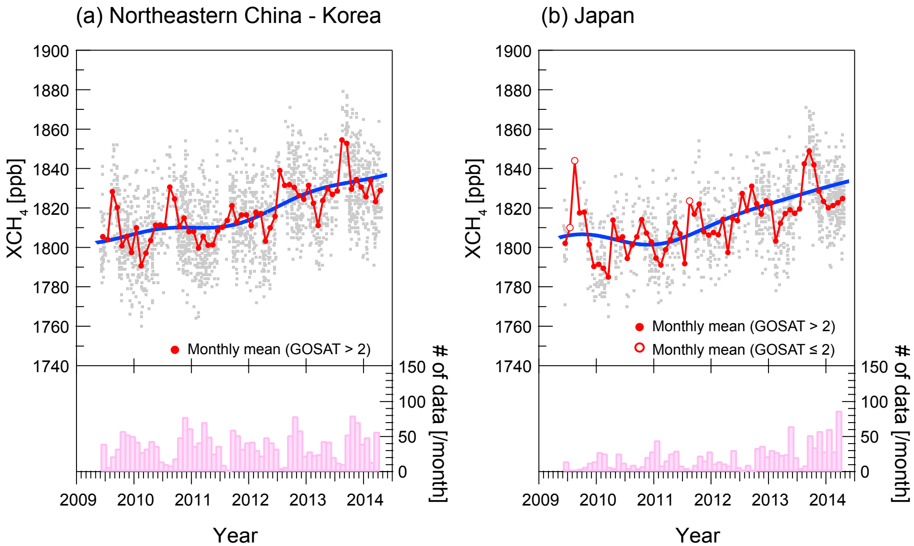

Figure 2. Temporal variations of GOSAT XCH_4 over the two regions of Northeast Asia: **(a)** Northeastern China-Korea (115–130° E, 30–40° N), and **(b)** Japan (130–145° E, 30–40° N). GOSAT XCH_4 data are shown in grey dot. The monthly means are plotted in red solid circle and line, whereas monthly means in open circles indicate less than two retrievals available per month. Blue lines indicate the long-term trends. The histogram in the bottom show the number of GOSAT XCH_4 data per month.

ACPD
15, 24995–25020, 2015

Large XCH_4 anomaly in summer 2013 over Northeast Asia observed by GOSAT

M. Ishizawa et. al.

Title Page
Abstract | Introduction
Conclusions | References
Tables | Figures
◀ | ▶
◀ | ▶
Back | Close
Full Screen / Esc
Printer-friendly Version
Interactive Discussion

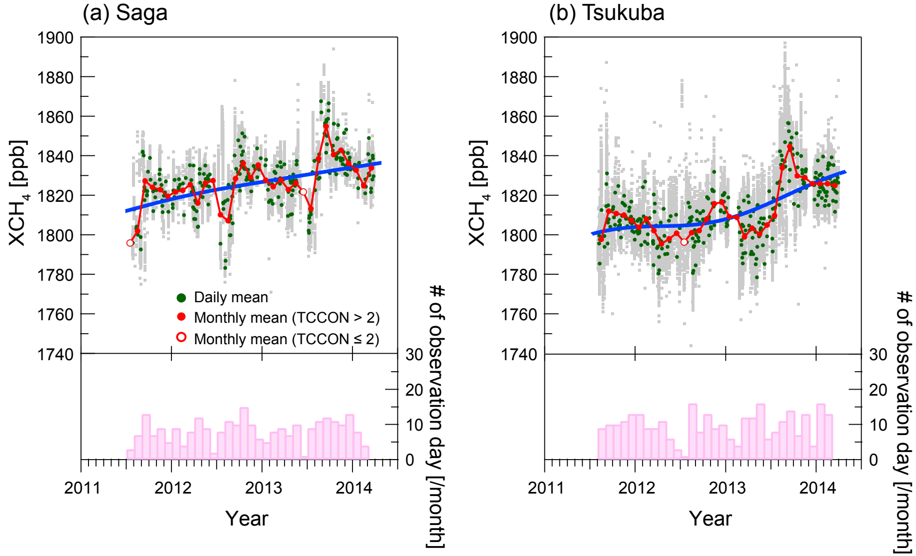

Figure 3. Temporal variations of TCCON XCH_4 at **(a)** Saga (130.29° E, 33.24° N) and **(b)** Tsukuba (140.12° E, 36.05° N), Japan. TCCON XCH_4 data are shown in grey dot, daily means in green dots. The monthly means are plotted in red solid circle and line, whereas monthly means in open circles indicate less than two retrievals available per month. Blue lines indicate the long-term trends. The histograms at the bottom show the number of observation day per month.

ACPD
15, 24995–25020, 2015

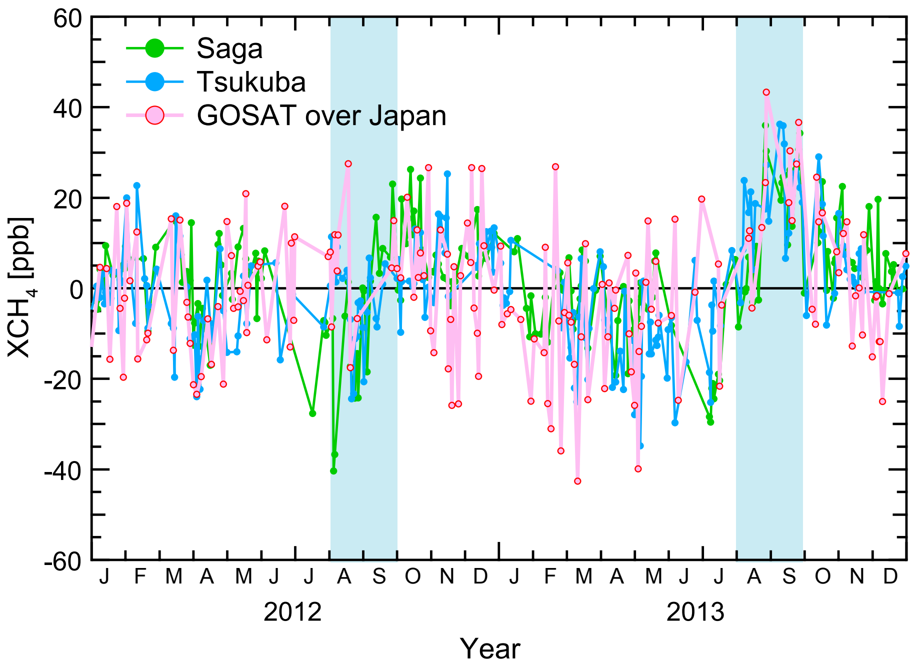

Figure 4. Detrended XCH_4 for 2012 to 2013 at Saga and Tsukuba, Japan and GOSAT over Japan. Long-term components in individual XCH_4 time series are removed by low pass digital filter of cutoff frequency of two years. August and September of both 2012 and 2013 are highlighted.

ACPD
15, 24995–25020, 2015

Large XCH_4 anomaly in summer 2013 over Northeast Asia observed by GOSAT

M. Ishizawa et. al.

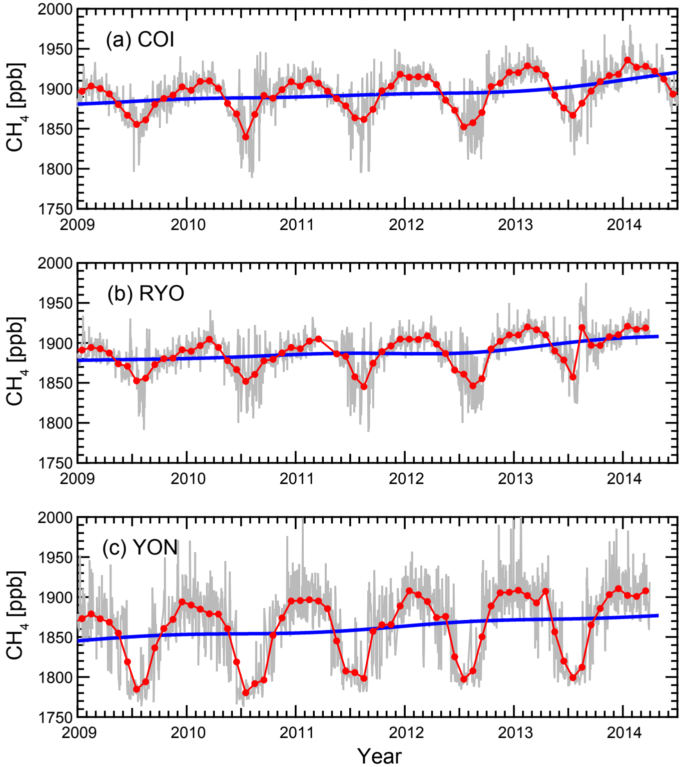

Figure 5. Temporal variations of atmospheric CH_4 concentrations observed at the ground-based monitoring sites around Japan, **(a)** Cape Ochi-ishi (COI, 43.16° N, 145.49° E), **(b)** Ryori (RYO, 39.03° N, 141.82° E), and **(c)** Yonagunijima (YON, 24.47° N, 123.02° E). The site locations are shown in Fig. 1. Afternoon means of hourly CH_4 concentrations are shown in grey lines. The monthly means are plotted in red solid circle and line. Blue lines indicate the long-term trends.

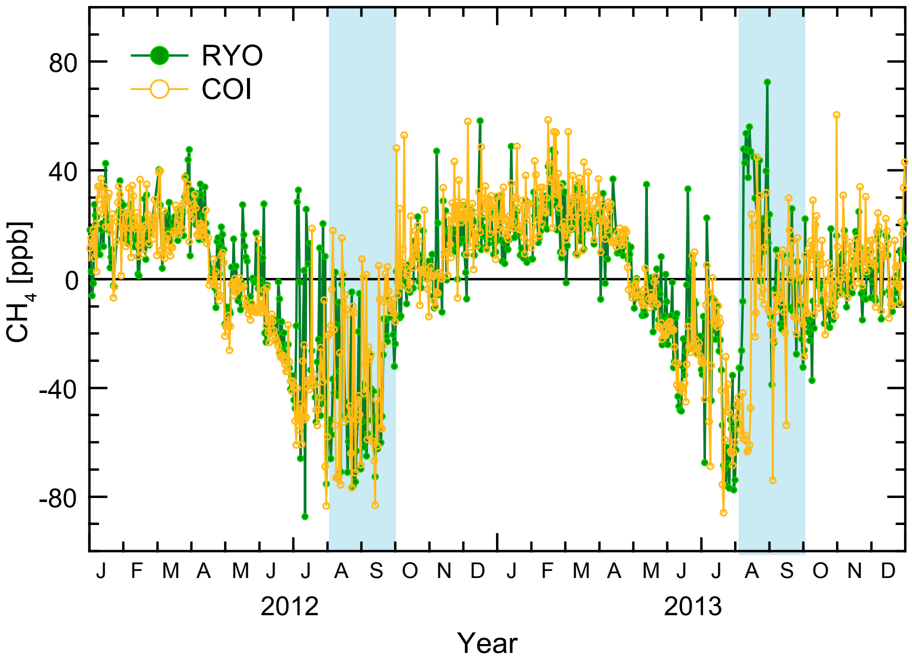

Figure 6. Detrended CH_4 for 2012 to 2013 at Ryori (RYO) and Cape Ochi-ishi (COI) in Japan. Long-term components in individual CH_4 time series are removed by low pass digital filter of cutoff frequency of two years. August and September of both 2012 and 2013 are highlighted.

ACPD
15, 24995–25020, 2015

Large XCH_4 anomaly in summer 2013 over Northeast Asia observed by GOSAT

M. Ishizawa et. al.

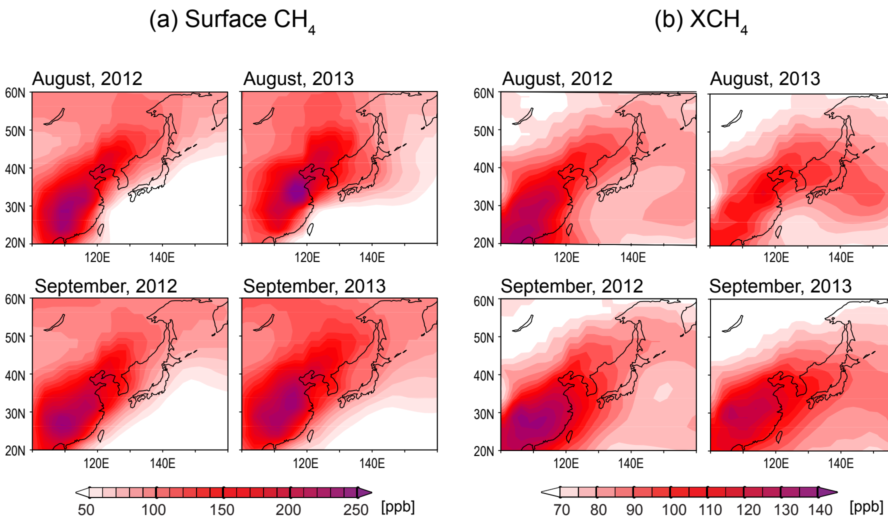

Figure 7. Spatial distribution of monthly mean modelled **(a)** CH_4 and **(b)** XCH_4 in August and September of 2012 and 2013, with respect to surface CH_4 and XCH_4 at South Pole, respectively.

ACPD
15, 24995–25020, 2015

Large XCH_4 anomaly in summer 2013 over Northeast Asia observed by GOSAT

M. Ishizawa et. al.

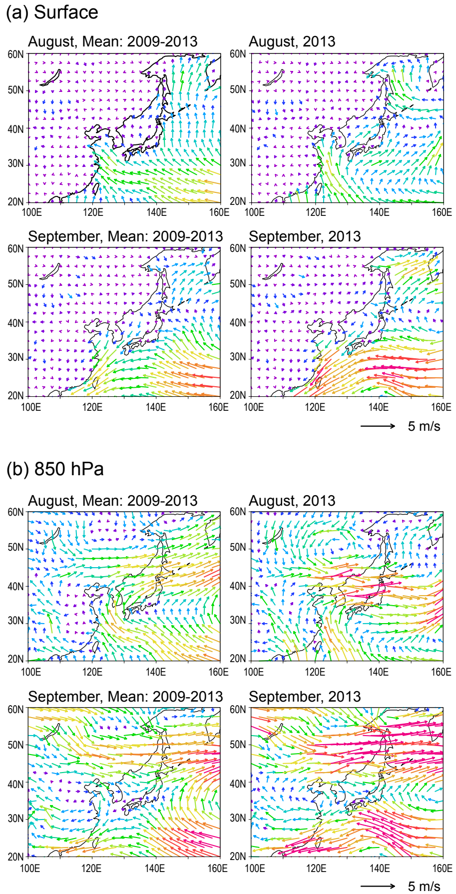

Figure 8. Monthly mean wind fields of August and September at **(a)** surface and **(b)** 850 hPa. The left panels are the wind fields averaged over the five years of 2009–2013, and the right panels are the monthly mean wind fields of the year 2013.

ACPD
15, 24995–25020, 2015

Large XCH_4 anomaly in summer 2013 over Northeast Asia observed by GOSAT

M. Ishizawa et. al.

Title Page
Abstract | Introduction
Conclusions | References
Tables | Figures
◀| |▶
◀ ▶
Back | Close
Full Screen / Esc
Printer-friendly Version
Interactive Discussion